Classification and Characterization of Objects from the GALEX and SDSS surveys

Luciana Bianchi[1], Mark Seibert[2], Wei Zheng[1], David A. Thilker[1], Peter G. Friedman[2], Ted K. Wyder[2], Jose Donas[4], Tom A. Barlow[2], Yong-Ik Byun[3], Karl Forster[2], Timothy M. Heckman[1], Patrick N. Jelinsky[6], Young-Wook Lee[3], Barry F. Madore[7], Roger F. Malina[4], D. Christopher Martin[2], Bruno Milliard[4], Patrick Morrissey[2], Susan G. Neff[9], R. Michael Rich[10], David Schiminovich[2], Oswald H. W. Siegmund[6], Todd Small[2], Alex S. Szalay[1], Barry Y. Welsh[6]

ABSTRACT

We use the GALEX (Galaxy Evolution Explorer) Medium Imaging Survey (MIS) and All-Sky Imaging Survey (AIS) data available in the first internal release, matched to the SDSS catalogs in the overlapping regions, to classify objects by comparing the multi-band photometry to model colors. We show an example of the advantage of such broad wavelength coverage (GALEX far-UV and near-UV, SDSS *ugriz*) in classifying objects and augmenting the existing samples and catalogs. From the MIS [AIS] sample over an area of 75 [92] square degrees, we select a total of 1736 [222] QSO candidates at redshift < 2, significantly extending the number of fainter candidates, and moderately increasing the number of

[1]Deptartment of Phys.& Astron., Johns Hopkins University,3400 N.Charles St., Baltimore, MD21218 (bianchi,zheng,dthilker,heckman,szalay@pha.jhu.edu)

[2]California Inst. of Technology,MC405-47,1200 E.California Blvd, Pasadena, CA91125 (mseibert,friedman,tab,krl,cmartin,patrick,ds,tas,wyder@srl.caltech.edu)

[3]Center for Space Astrophysics, Yonsei University, Seoul 120-749, Korea (byun,ywlee@obs.yonsei.ac.kr)

[4]Laboratoire d'Astrophysique de Marseille, BP8, Traverse du Siphon, 13376 Marseille Cedex 12,FR (denis.burgarella,roger.malina,bruno.milliard@oamp.fr)

[6]Space Sciences Laboratory, University of California at Berkeley, 601 Campbell Hall, Berkeley, CA 94720 (patj,ossy,bwelsh@ssl.berkeley.edu)

[7]Observatories of the Carnegie Institution of Washington, 813 Santa Barbara St., Pasadena, CA 91101 (barry@ipac.caltech.edu)

[9]Laboratory for Astronomy and Solar Physics, NASA Goddard Space Flight Center, Greenbelt, MD 20771 (neff@stars.gsfc.nasa.gov)

[10]Department of Physics and Astronomy, University of California, Los Angeles, CA 90095 (rmr@astro.ucla.edu)

bright objects in the SDSS list of spectroscopically confirmed QSO. Numerous hot stellar objects are also revealed by the UV colors, as expected.

Subject headings: galaxies:statistics —stars: statistics —surveys:ultraviolet — surveys:optical —QSO

1. Introduction

The GALEX (Galaxy Evolution Explorer) mission is providing the first UV sky surveys with wide area coverage and deep sensitivity, in two UV bands, far-UV (FUV) and near-UV (NUV). The major science objectives and characteristics of GALEX, and of the surveys, are described by Martin et al (2004).

The portions of the Medium Imaging Survey (MIS) and All Sky Imaging Survey (AIS) completed at the time of the Internal Release 0.2 (Morrissey et al. 2004) substantially overlap with the Sloan Digital Sky Survey (SDSS) imaging and spectroscopic optical surveys, for a total 72 and 92 square degrees respectively. We present in this work examples of analyses of the color-color digrams which illustrate the advantages of combining two UV bands and five optical bands, in classifying and characterizing objects of certain types, and within certain parameter ranges. We classify the matched GALEX and SDSS sources by comparing their observed colors to model colors.

This paper complements the work by Seibert et al. (2004), which presents a statistical analysis of the magnitude distributions in the correlated GALEX and SDSS sample, and of the characteristics of objects with previously available classification within the sample. Several other papers in this issue derive statistical properties of galaxies from this sample (alone or correlated to catalogs in other wavelength bands), e.g. Buat et al. (2004), Budavari et al. (2004), Arnouts et al. (2004), Treyer et al. (2004), Yi et al. (2004), Salim et al. (2004), Rich et al. (2004). Some of these works basically adopt in the definition of the sample the star/galaxy classification provided by the SDSS pipeline, which define as "star" a source appearing point-like at the SDSS resolution, and as "galaxy" an extended source. Also, these works are mainly focused on color-magnitude diagrams and luminosity functions, while the present analysis is focused on the interpretation of color-color diagrams.

2. The sample and the Analysis

The GALEX on-orbit performance is described by Morrissey et al. (2004). GALEX FUV (1350–1750 Å) and NUV (1750–2750 Å) imaging is used in this work, with optical imaging from the SDSS in the *ugriz* bands.

In the current GALEX Internal Data Release, IR0.2, the matched GALEX+SDSS surveys cover a non-contiguous area of the sky (excluding overlaps) of 75 square degrees (MIS) and 92 square degrees (AIS). The MIS has exposure times varying between 1000 and 1700 sec., yielding a magnitude limit (1 σ) of 22.6 (FUV) and 22.8 (NUV), in the AB magnitude system, while the AIS has typical exposure time of about 100 sec, corresponding to limiting magnitudes FUV $\approx$ 20. and NUV $\approx$ 20.8. More relevant to the analysis that will follow is the number of sources within each survey with photometric errors better than specific limits in any band. These numbers are compiled in Table 1, and can be compared to the total number of sources in these surveys, given in Table 1 of Seibert et al (2004). Table 1 shows that the GALEX MIS survey in the NUV band is somehwat deeper than the SDSS imaging survey, as is the GALEX Nearby Galaxies Surveys (NGC) that has a similar exposure time (Bianchi et al. 2004).

For a description of the matching procedure between GALEX and SDSS sources, see Seibert et al. (2004). Because of the different spatial resolutions, 4.5/6″ (GALEX FUV/NUV) and 1-2″ (SDSS), some GALEX sources have more than one optical counterpart. We excluded from our analysis the sources with multiple matches (even when the second match was farther away and the first match is probably significant), because the source colors may not be meaningful, due to potential contamination from other sources unresolved by GALEX. This restriction excludes about 17% (MIS) and 18% (AIS) of the sources from the analysis. This factor must be taken into account when considering the numerical population density (i.e. sources per square degree) and when comparing with other catalogs, and other papers in this volume.

The accuracy of the GALEX calibration is described by Morrissey et al (2004). The magnitudes of the IR0.2 release are tied to the ground-based calibration. The calibration is currently being improved with on-going observations of standard stars, and appears to be accurate within 0.1 mag. Taking into consideration several factors, we restricted our sample for the analysis to sources with photometric errors (excluding the zero-point error) better than 0.1/0.15 mag (GALEX NUV/FUV bands) and better than 0.05 mag (SDSS bands). We also consider a less stringent error cut (0.2 mag in any band) for consistency with Seibert et al. (2004), and give results for both error cuts.

3. The models

We computed model colors for different astrophysical objects, in the GALEX and SDSS bands, by using the transmission curves of the GALEX and SDSS filters available from the web sites of the projects. For normal stars, we used fully blanketed Kurucz models, with $T_{\rm eff}$ from 50000 K to 3000 K, from the grids of Bianchi & Garcia (in preparation) and Lejeune et al. (2002). Only models for log g = 5.0 are shown in figure 1, to avoid crowding. A WD model for $T_{\rm eff}$=135,000 K, computed with the TLUSTY (Hubeny & Lanz 1995) code, is also shown. WD models for lower $T_{\rm eff}$ overlap with the hottest main sequence star colors, thus are not shown.

Colors for integrated populations were computed from Bruzual & Charlot (2003) models, for the two extreme cases of Single-burst Star Formation (SSP) and Continuous Star Formation (CSP). We used both Salpeter, and Chabrier (2003) Initial Mass Functions (both cases are plotted, but are almost indistinguishable), with a range of initial masses 0.1-100$\mathcal{M}_{\odot}$. Only solar metallicity models are shown in the plots.

For QSO spectra, we use a modified composite spectrum of Francis et al. (1991). At restframe wavelengths shortward of 1000 Å, the power law is $f_{\nu} \propto \nu^{-1.8}$ (Zheng et al. 1997). The absorption effect of $Ly\alpha$ absorption follows the work of Press & Rybicki (1993).

Models were also reddened with different types of extinction (only MW-type extinction is shown in the plots). The reddening arrows for the different model points are not exactly parallel, because we reddened the model spectra and then applied the filter transmission curves, which is more accurate than applying an extinction value appropriate to the λ_{eff} of the filter.

The extensive grids of model colors will be published elsewhere (Bianchi et al., in prep).

4. Analysis. Results and conclusions

In Figure 1 we show two examples of color combinations, that illustrate three different advantages of using UV plus optical bands. First, the UV colors of starburst (SSP) populations younger and older than approximately 10^9 yrs are ambiguous (as age indicators) because of the UV upturn of the old population. The age ambiguity is largely removed when using an optical band, e.g. V, as shown in our example by the NUV-r color.

In the spectro-photometric determination of ages (and intrinsic luminosities, thus masses) of SSP populations (stellar clusters, or starburst galaxies), extinction must be determined concurrently with the physical parameters of the source, mainly the age, since both age and

extinction affect the observed slope. Similarly, one can derive concurrently $T_{\rm eff}$ and extinction from the photometric SED of stars (e.g. Bianchi et al. 2001). The second advantage clearly visible in all panels of Figure 1 is that, while fluxes at UV wavelengths suffer by the selective extinction more than optical fluxes, the *color* FUV-NUV is essentially reddening free (for a typical Galactic extinction law with R_v=3.1, as used in Figure 1, and for moderate amounts of reddening). Therefore, the age of an SSP population can be determined from this color independently from the estimate of reddening (see also Bianchi et al 2004), once the ambiguity between young and old ages is resolved by the additional optical band.

The third advantage shown by Figure 1 (lower panels) is that QSOs at low redshift (<2) can be separated from the stars by their color. This is discussed in more detail in the next section. Also, stars of certain types can be separated, and easily identified, by different color combinations (see also Bianchi & Martin 1998).

4.1. Low-Redshift QSO Candidates

In the lower panels of Figure 1 we separated the point-like sources which lie on the left-hand side of the envelope defined by the stellar model colors. In this region lie the QSO model colors for low redshift, and about half of the spectroscopically confirmed QSO SDSS sample. With our stringent error cuts specified above, we find 548 QSO candidates in the MIS sample. Of these, 221 are spectroscopically confirmed QSOs by the SDSS survey. Scaling this number by the SDSS QSO confirmation rate, 75% at low z (Richards et al. 2002) the number of SDSS "candidates" in the same color space becomes 295. If we relax the error cut to 0.2 mag in all bands (for comparison with Seibert et al. 2004, this issue) the numbers become: 1736 low redshift QSO GALEX candidates, 263 of which spectroscopically confirmed.

For the AIS, which covers at shallower flux limits 92 square degrees, we find, with the same stringent error limits, 99 low redshit QSO candidates, of which 45 are included in the SDSS spectroscopically confirmed sample. However, these error cuts limit the number of sources to about 900, out of the total almost 100,000. Using error cuts of 0.2 mag for all bands, we retain about 2100 AIS sources, and the number of low redshift QSO candidates becomes 222, of which 91 are spectroscopically confirmed.

Our color-selected sample therefore increases the number of QSO candidates in the redshift range $z < 2$. However, we stress that our photometric selection of objects, defined as the points outside (left of) the models for single stars in the color-color plot, may also include binary stars. The distribution of redshifts within the spectroscopically confirmed

SDSS sample is shown by Seibert et al. (2004, this issue).

In Figure 2 we show the characteristics of the GALEX-selected low redshift QSO-candidate samples versus the spectroscopically confirmed subset. To evaluate the significance of our candidate sample, we plotted in Figure 2 (left, dotted line) also the subsample of QSOs candidates brighter than 19.1 in the *i*-band, which is the completeness limit of the low-z QSO (z<3) SDSS spectroscopic sample, according to Richards et al. (2002). The histograms in Figure 2 show that *(i)* the GALEX-AIS photometrically selected sample overlaps the magnitude range of the SDSS spectroscopic QSO sample, and is numerically larger by less than a factor of two, taking into account the SDSS confirmation rate, *(ii)* the MIS photometrically selected sample significantly extends to lower magnitudes. In the range of magnitude overlap with the SDSS spectroscopic survey, the GALEX-MIS selected sample is still more numerous by 50% or less. In conclusion, our photometric selection of low redshift QSO candidates is significantly extending the number of candidates to fainter magnitudes, in comparison to the SDSS spectrscopic sample, and slightly increases the number of bright candidates.

The most prominent spectral feature in QSOs' spectra is the flux break due to the accumulated Lyα forest absorption. At redshift $z < 2$, this feature is shortward of the SDSS range, and SDSS uses the general power-law shape at longer wavelengths to search for QSOs, without the Lyα break. GALEX has the advantage of detecting this feature in the UV bands, thus complements the SDSS in its quasar search. With a large number of new QSO candidates, GALEX demonstrates the potential of finding many more, fainter quasars, improving our measurement of the QSO luminosity function at $z < 2$.

4.2. The Stars in the MW Halo

The numerical advantage of spectro-photometric classification over the SDSS spectroscopic sample is greater for stellar objects (Figure 1). An additional result is the derivation of extinction maps in the MW, which will be the subject of a future paper. For instance, in the MIS IR0.2 sample, we have about 2000 stellar objects (errors < 0.2 mag) in 75 square degrees, i.e. about 27 per square degree. In a forthcoming paper we will use seven bands (GALEX plus SDSS) to derive concurrently extinction and $T_{\rm eff}$ by comparison to model colors, following a modification of the method by Bianchi et al (2001), implemented by Bianchi and Tolea (2004, in preparation) for HST photometry. Very hot stellar objects are, as expected, easily identified by the UV colors (Figure 1). Seibert et al. (2004) present a preliminary discussion of specific classes of stellar objects that emerge from GALEX plus SDSS photometric diagrams.

Acknowledgement:

GALEX (Galaxy Evolution Explorer) is a NASA Small Explorer, launched in April 2003. We gratefully acknowledge NASA's support for construction, operation, and science analysis of the GALEX mission, developed in cooperation with the Centre National d'Etudes Spatiales of France and the Korean Ministry of Science and Technology. LB is very grateful to J. Maiz, M. Garcia, J. Herald for help in constructing the stellar models, and to S. Yi and T.Budavari for helpful discussions.

REFERENCES

Arnouts, S., et al. 2004, ApJL, this issue

Bianchi, L., et al, 2004, ApJL, this issue

Bianchi, L., Madore, B., Thilker, D., Gil de Paz, A., and Martin, C., 2004a, in "The Local Group as an Astrophysical Laboratory", in press

Bianchi, L., Madore, B., Thilker, D., Gil de Paz, A., and the GALEX team, 2004b, AAS 203, 91.12

Bianchi, L., and Garcia, M., 2004, in preparation

Bianchi, L., Scuderi, S., Massey, P., and Romaniello, M. 2001, AJ, 121, 2020

Bianchi, L., & Martin, C., 1998, in "UV Astrophysics beyond the IUE Final Archive", eds. R. Gonzalez-Riestra, W.Wamsteker and R.A. Harris, ESA SP-413, p. 797

Bruzual, G. & Charlot, G., 2003, MNRAS, 344, 1000

Buat, L., et al, 2004, ApJL, this issue

Budavari, L., et al, 2004, ApJL, this issue

Chabrier, G., 2003, PASP, 115, 763

Francis, P.J., et al. 1991, ApJ, 373, 465.

Hubeny, I. & Lanz, T. 1995, ApJ, 493, 875

Lejeune, T., Cuisinier, F., & Buser, R. 1997, A&AS, 125, 229

Martin, D. C., et al. 2004, ApJ, present volume

Morrissey, P., et al. 2004, ApJ, present volume

Press, W.H. & Rybicki, G.B. 1993, ApJ, 418, 585

Richards, et al. 2002 AJ 123, 2945

Rich, M. et al. 2004, ApJL, this issue

Salim, S. et al. 2004, ApJL, this issue

Seibert, M. et al. 2004, ApJL, this issue

Schlegel, D. J., Finkbeiner, D. P., & Davis, M. 1998, ApJ, 500, 525

Yi, S. et al, 2004, ApJL, this issue

Zheng, W. et al., 1997, ApJ, 475, 469

Table 1. The sample of sources in the different bands

Band	No. Sources (error<0.2 mag)	No. Sources (error<0.1 mag)	No. Sources (error<0.05 mag)
	MIS Total Sources		
FUV	40355	8181	1527
NUV	229452	127253	27905
u	53747	41468	32947
g	143432	90350	62221
r	169519	108808	70245
i	144014	91459	61190
z	73075	50203	38709
	AIS Total Sources		
FUV	3835	572	113
NUV	32129	7291	1041
u	42064	33714	28288
g	74523	62889	48277
r	76750	66673	51821
i	72309	59527	45681
z	50227	38400	30508

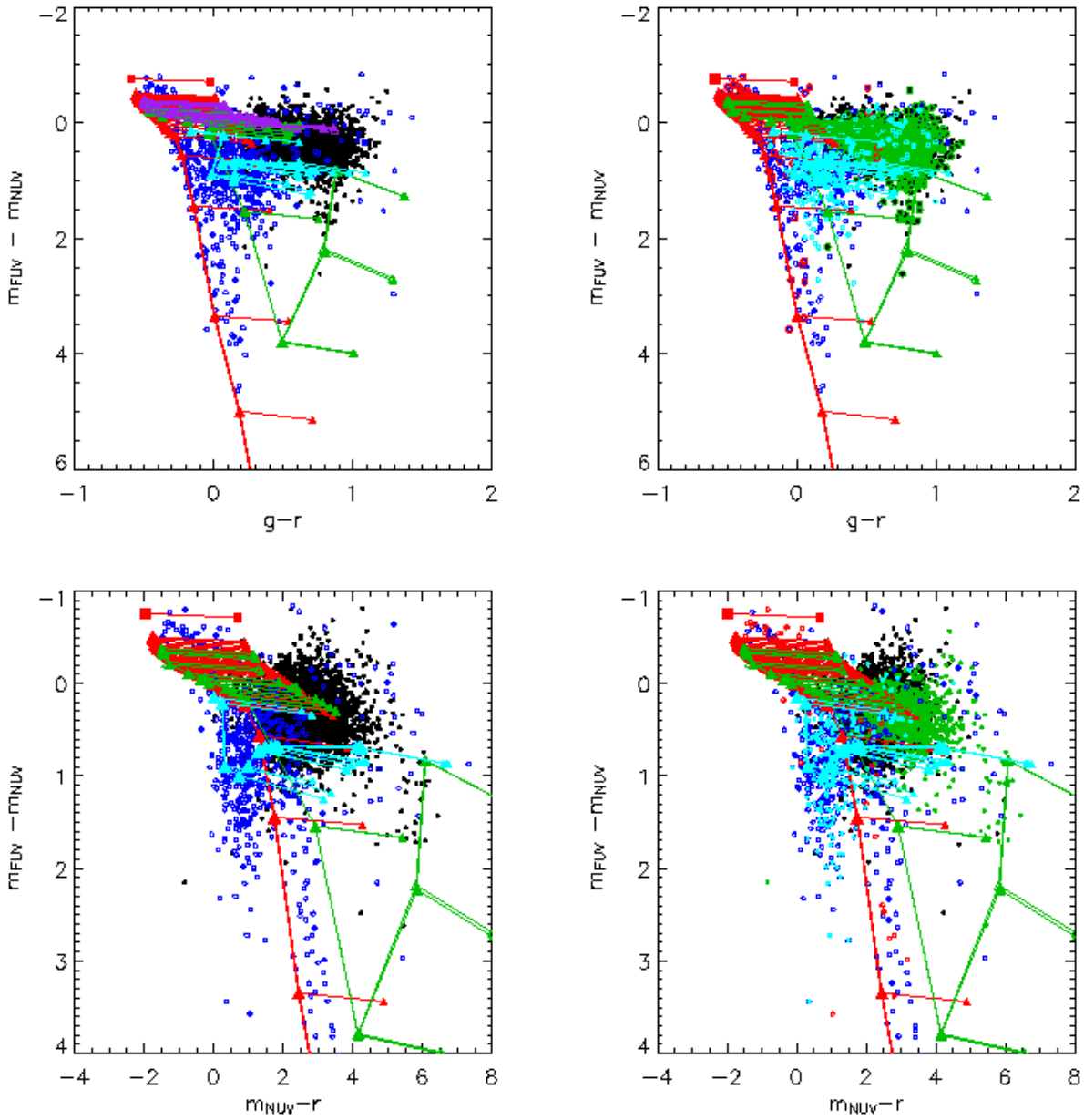

Fig. 1.— Two color-color diagrams for GALEX IR0.2 MIS sources matched to the SDSS DR1 sources. Sources classified as point-like in the SDSS catalog (SDSS type: "star") are the blue circles, sources extended in the SDSS (SDSS type: "galaxy") are plotted as black points. On the right-hand panels, the objects with *spectroscopic* classification from the SDSS survey are shown in red (stars), turquoise (QSOs) and green (galaxies). Model colors are indicated as: red (dark) triangles: stellar models, from $T_{\rm eff}$=50000K (uppermost point) to 3000K, red square: WD with $T_{\rm eff}$=135,000K; green triangles: integrated stellar population (Single Star Burst, SSP) models, from age 0.5Myr to 10 Gyr, and purple triangles: Continuous Star Formation (CSP) models for the same ages (shown only in the top left panel); turquoise triangles: QSOs in the redshift range 0-4. Reddening arrows corresponding to E(B-V)=0.5 (MW reddening, R_v=3.1) are shown for each model point. Top panels: NUV-FUV vs g-r. It is evident that the classification star/galaxy based on the source PSF is roughly a good division, however QSO (mostly point-like) fall in the "star" class. The top (right)

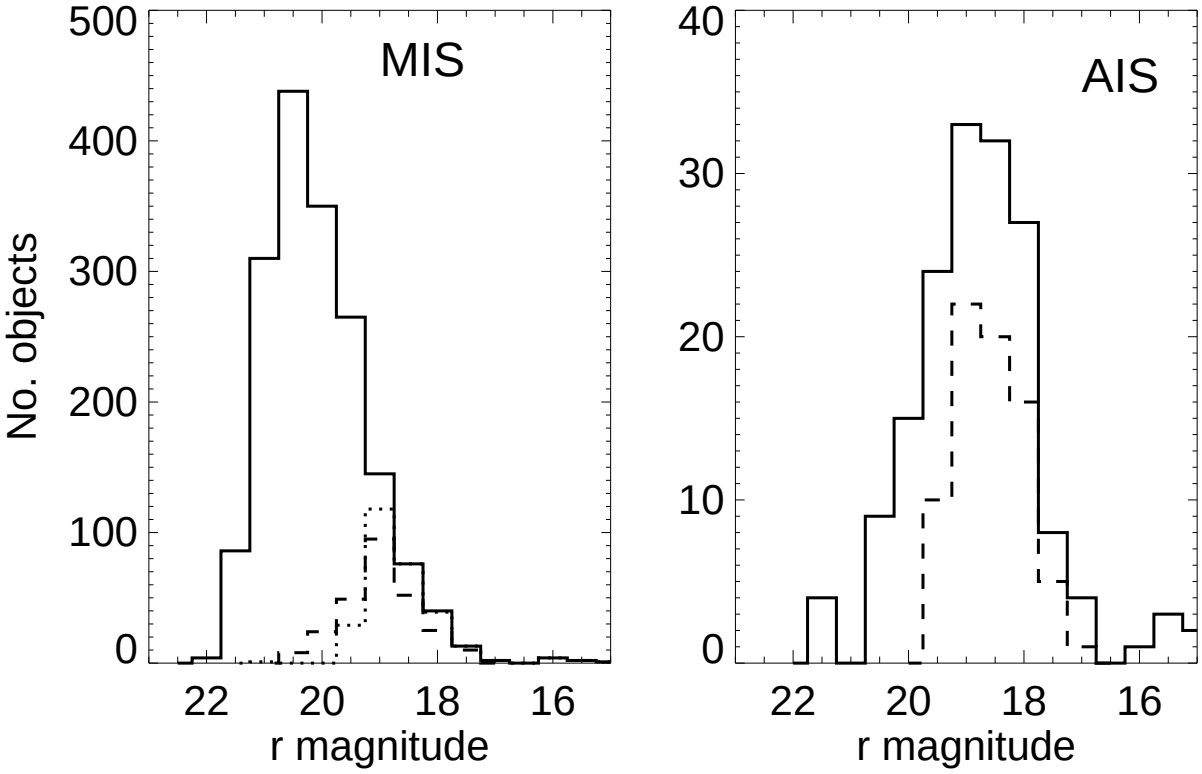

Fig. 2.— Histograms (r-band magnitude) of low redshift QSO candidates, selected photometrically from from the MIS (left) and AIS (right) IR0.2 surveys. The dashed histograms are the subset of the selected samples that are spectroscopically confirmed in the SDSS survey. The dotted histogram is the subset of the MIS sample with i <19.1 mag (see text).